

Short communication

Low temperature synthesis and characterization of nanoscale Cu_6Sn_5 particles as lithium anode material

Mladen Mladenov^{a,*}, Petya Zlatilova^a, Iovka Dragieva^a, Kenneth Klabunde^b

^a Institute of Electrochemistry and Energy Systems, Bulgarian Academy of Sciences, 1113 Sofia, Ac. G. Bonchev Bl.10, Bulgaria

^b Kansas State University, Manhattan, KS 66506, USA

Available online 8 September 2005

Abstract

The current article displays the possibilities of borohydride reduction method, carried out at room temperature and ambient atmospheric condition, to be a technological process for large scale production of Cu_6Sn_5 nanoparticles. This composition is very attractive recently via anode material in secondary lithium batteries. The content changes of prepared nanoparticles depend on the initial ratio of metal salt solutions and the concentration of complex forming agent used. One hypothesis is draw out on the basis of experimentally analyzed content of electrodes, interrupted at various potentials of the first charge cycle: 690 mV, 540 mV, 200 mV and 10 mV. Thus, the good life cycle of these nanoscale systems is a result of an intercalation of lithium occurring during phase transition from *hcp* to *fcc* of the lattice.

© 2005 Elsevier B.V. All rights reserved.

Keywords: Lithium; Anode

1. Introduction

In recent years, many authors [1–9] have been working upon alternative anode materials for secondary lithium batteries. Different metals (Al, Pb and Sn) and intermetallic compounds as Cu_6Sn_5 , Sn–SnSb, Ni–Sn, SnAg and $\text{Sn}_2\text{Fe–C}$ have been investigated as potential perspective anode materials, and some of them possess higher specific capacity than the one of the applied up to the present graphite and other carbon materials. However, the problems with the volume changes resulting from the phase transitions have not yet been solved.

In 1999, Kepler et al. discovered that lithium could be intercalated into the Cu_6Sn_5 alloy forming the system $\text{Li}_x\text{Cu}_6\text{Sn}_5$ [1]. Thus, this is a material with a theoretical gravity capacity of about 350 mAh g^{-1} , and with significantly higher volume capacity, corresponding to 1656 mAh ml^{-1} , in comparison with the commercial LiC_6 [1].

According to Ref. [2], the reaction of lithium insertion into the copper–tin compound proceeds in two stages. At the beginning lithium is intercalated into the hexagonal lattice (NiAs-type structure, $P6_3/mmc$) of the initial Cu_6Sn_5 alloy to the phase $\text{Li}_x\text{Cu}_6\text{Sn}_5$. The same is an *iso*-structure of the cubic symmetry phase Li_2CuSn (Cu_2MnAl -type, $Fm/3m$). The authors have experimentally clarified that more precisely and stoichiometrically expressed this is the phase $\text{Li}_{2.17}\text{CuSn}_{0.83}$. The second stage of the intercalation process of Li into the compound leads to a “disordered” $\text{Li}_{4.4}\text{Sn}$ phase—a process joined by the separation and observation of nanoscale grains of Cu [2].

Yang et al. [3] propose the preparation of anode mass for lithium batteries with content Sn and Sn–Sb, combining microsized powders with nanosize particles obtained by the borohydride reduction method from aqueous $\text{SnSb}_{0.14}$ solutions.

In a subsequent work, Yang et al. [4] started to use only nanosize particles but with different dispersion, from the Sn and Sn–SnSb contents, which were again obtained by the borohydride method. They achieve the best charge capacity for the intercalation of 1.6 mol Li per mol active material for the above-mentioned content.

* Corresponding author. Tel.: +359 2 9792737; fax: +359 2 722 544.

E-mail addresses: mladen47@bas.bg (M. Mladenov), iovka@cleps.bas.bg (I. Dragieva), kenjk@ksu.edu (K. Klabunde).

By using the same low temperature synthesis and reduction with sodium borohydride of copper and tin aqueous salt solutions Kim et al. [5] synthesized Sn–Cu–B alloy, which they investigated as anode for secondary lithium batteries.

According to them [5], the cycleability of a Cu_6Sn_5 electrode synthesized as nanoscale material is significantly enhanced in comparison with the properties of the same material prepared by sintering or mechanical alloying.

Our team has significant experience in the synthesis, characterization and use of nanosize materials, including those, prepared by the low temperature borohydride (BH) method, which comprises the use of aqueous solutions of metal salts or complexes with sodium borohydride reductor [6–8]. Lately, we have been actively engaged in the development of intermetallic nanoscale systems and their production and application in electrochemical power sources, while we also have paid attention to the system Cu_6Sn_5 [9]. The current work aims at displaying our possibilities for refinement of the synthesis in order to achieve maximum precision of the chemical content, together with high reproducibility by form and size of the obtained nanoparticles. Another aim was to qualitatively and quantitatively follow this nanosystem's lithiation mechanism and to observe its possibility as anode material for secondary lithium batteries.

2. Experimental

The BH-method synthesis proceeds in a regime of ideal mixing of two solutions. One of them contains dissolved metal ions in given ratios and the other one—sodium borohydride. The precursors are the copper and tin salts $\text{CuCl}_2 \cdot 2\text{H}_2\text{O}$ and $\text{SnCl}_2 \cdot 2\text{H}_2\text{O}$, respectively. NaBH_4 was used as reducing agent and sodium citrate was the complex forming agent one. The pH values of the initial solutions, of the solution after the carried out synthesis and of the filtrate after separation of the synthesized nanoparticles are determined, as well as the pH of the filtrate after their continuous washing with distilled water. After precisely removing the anions, the pure precipitate is washed out with ethyl alcohol and is dried in a vacuum drier.

Syntheses with various ratios of the two metals and different quantity of the applied complex forming agent were also carried out. In order to meet the needs of comparative determinations and evaluations pure nanoparticles containing only tin or only copper were also synthesized by BH method. Table 1 presents data for all nanoparticles subjected to physicochemical and electrochemical characterization, and to the discussions in the current work.

The boron quantity, which does not exceed 0.15 wt% in all samples, was analytically determined. The specific surface area is determined by the BET method and the obtained values for the synthesized Cu_6Sn_5 particles are in the range from $25 \text{ m}^2 \text{ g}^{-1}$ to $42 \text{ m}^2 \text{ g}^{-1}$.

Philips APD-15 diffractometer was used for the routine X-ray diffraction tests. SEM investigations were carried out with an electron microscope JEM 200 CX of JEOL, Japan. The copper and tin quantitative content in the synthesized initial powders is determined with X-ray microanalyzer JEOL Superprobe 733. With this piece of equipment we performed an investigation of the distribution throughout the phases as a composition (in COMPO regime, EDAX) of the electrode samples, which underwent electrochemical lithiation. We tried to estimate for these samples the quantity of intercalated lithium at the different regimes by analyzing the heavy atoms bonding with lithium, atom with atom, as a compound in the working electrolyte. We intend to improve and develop this set of methods especially for investigation of membrane electrodes.

The electrode mixture is prepared by the synthesized nanoparticles and teflonized acetylene black TAB-2–30%. Initially, the mixture is dispersed in a liquid medium of organic solvent, and then it is dried in a vacuum at 60°C temperature. From the dried powder-like mixture a paste is prepared with propylene carbonate (PC) or *N*-methyl pyrrolidone, it is pasted upon a copper plate 15 mm in diameter and is pressed. The prepared electrodes are dried in vacuum at temperature up to 60°C for 2 h.

In Fig. 1(a), the surface of the thus prepared electrode is observed, and in Fig. 1(b) the cross-section of the same electrode, prepared by Cu_6Sn_5 particles according to the synthesis and denoted with number #2257 in Table 1, can be seen.

Table 1
Experimental data of synthesized Cu_xSn_y nanoparticles by BH reduction

Sample #	Synthesis #	Complex citrate ($\text{g} (100 \text{ ml})^{-1}$)	Analytical results		Ratio Cu/Sn (at% vs. at%)	XRD spectra
			Cu (at%)	Sn (at%)		
1	2256	–	–	100	–	Fig. 2(a)
2	2273	–	100	–	–	Fig. 2(f)
3	2250	–	–	–	1.20 ^a	Fig. 2(b)
4	2320	2.94	56.83	42.00	1.35	–
5	2321	5.88	58.75	41.25	1.42	Fig. 2(d)
6	2322	8.82	58.66	40.75	1.44	–
7	2326	5.88	61.15	38.85	1.57	Fig. 2(e)
8	2327	5.88	54.47	44.36	1.23	–
9	2316	2.94	56.44	43.56	1.29	–
10	2257	2.94	55.99	47.01	1.27	Fig. 2(c)

^a This is a ratio between atomic percent of metals of initial salts solutions for the BH synthesis.

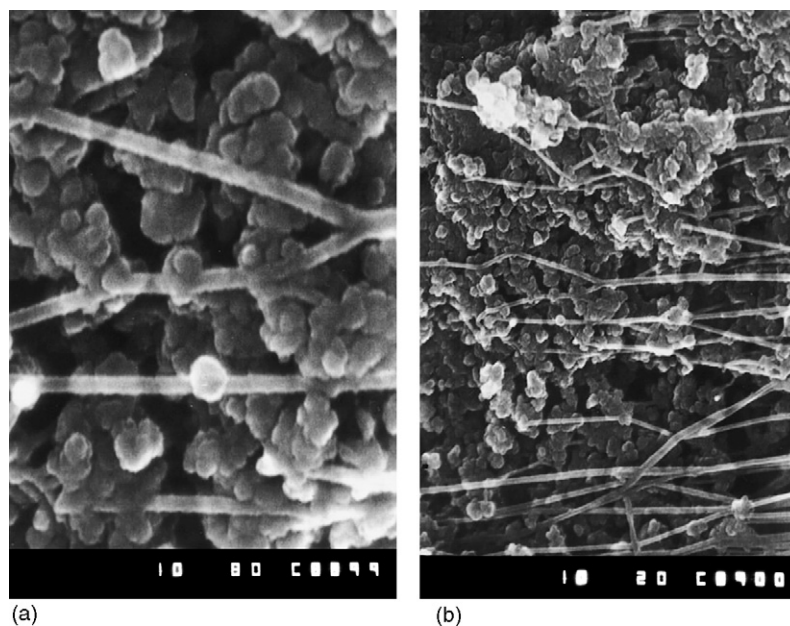


Fig. 1. (a) SEM morphology—a surface of the electrode prepared from sample 10 (synthesis #2257, Table 1) and (b) SEM morphology—a cross-section of the electrode prepared from sample 10 (synthesis #2257, Table 1).

The electrodes are tested in laboratory electrochemical cells from the type: Li//1 M LiClO₄, PC/EC (1:1)//Cu₆Sn₅. The cells are cycled in galvanostatic mode at current densities $C/10$ and in the potential range from 1.3 V to 0.01 V, the reference electrode being Li/Li⁺. The qualitative and quantitative phase changes of the electrode-composite during its lithiation in the first cycle are followed at selected different potential levels up to 0.680 V, to 0.54 V, to 0.2 V and to 0.01 V, respectively.

3. Results

3.1. Synthesis of different composition Cu_xSn_y nanoparticles

Table 1 presents the various contents of Cu_xSn_y nanoparticles synthesized by the borohydride method. When sodium citrate in different concentrations is used as complex forming agent it is possible to obtain Cu_xSn_y nanoparticles without oxides or other unwanted impurities—samples 5, 7 and 9. The increase of the complex forming agent concentration (samples 4–6) while preserving the tin/copper ratio in the initial solutions has a selective effect on the concentration of the cations participating in the reduction process and also leads to increase in the copper content and decrease in the tin one in the synthesized nanoparticles, due to the bonding of tin in a complex.

On the other hand, when preserving a constant concentration of the complex forming agent it is possible by correction of the ratio between the copper and tin salts to obtain nanoparticles with varying content from the ratio Cu/Sn = 1.23 to 1.42 or 1.57 for samples #8, 5 and 7, respectively. Impurities from

oxides were analyzed for the samples #4, 6 and 8, reaching about 1%.

From the presented in Table 1 data, it is obvious that the low temperature method of nanoparticles synthesis using sodium borohydride for the reduction of metal aqueous salts solutions is a technology for the production of Cu₆Sn₅ nanoparticles. Via this technology, we can well control the content and highly reproduce by size and shape the nanoparticles. It is clear that the technique (see Fig. 1(a and b)) for electrodes preparation and their subsequent standard characterization is also reliable. The performed comparisons on the synthesized particle size according to the determination of their specific surface area (SSA) and via patterns made with TEM and SEM tests displayed a fair correspondence into the range of 20–45 nm.

3.2. XRD investigations of Cu_xSn_y nanoparticles

A series of X-ray diffractions are presented in Fig. 2 and the spectra of a pure tin—Fig. 2(a) and of a pure copper—Fig. 2(f), synthesized by the borohydride method, are given for comparison. In case of synthesis with selected copper/tin ratio 1.20^a as with the Cu₆Sn₅ alloy in Fig. 2(b and c), the effect of the complex forming agent, which complicates and decreases the content of the tin free phase, can be observed.

When using one and the same complex forming agent concentration the increase of the copper content from ratio 1.42 (Fig. 2(d)) towards 1.57 (Fig. 2(e)) leads to the appearance of the phase εCu₃Sn.

Precise XRD investigations were carried out [5], including by us [9] for that system on the phase transitions pass during long-term cycling.

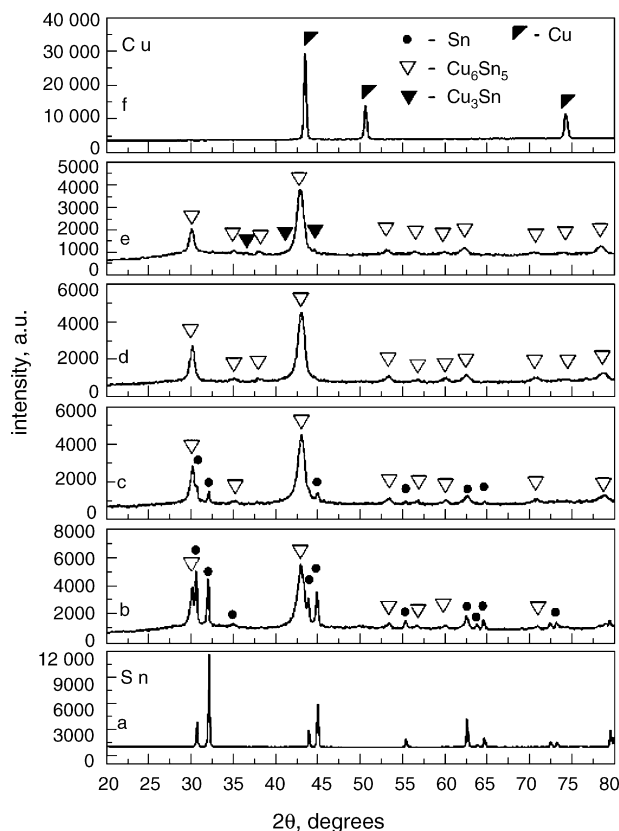


Fig. 2. XRD spectra of: (a) pure Sn, (b) #2250, (c) #2250, (d) #2321, (e) #2326 and (f) #2273.

3.3. Effect of the lithiation upon the morphology, phase and composition changes in $\text{Li}_n\text{Cu}_x\text{Sn}_y$ electrodes

The dependence of voltage versus specific capacity for the first cycle (Li insertion) into Cu_6Sn_5 electrode at a current corresponding to $C/10$ is given in Fig. 3. To investigate the phase transitions, the compositional morphology and chemical content of the electrode during the process of Li intercalation we interrupted the lithium intercalation process at various potentials (690 mV, 540 mV, 200 mV and 10 mV).

The precise XRD investigations on phase formation of the shown above examples have been presented and will be published soon [10].

In Fig. 4(a), the SEM morphology of the electrode surface is presented and right next to it is a photo in COMPO regime—EDAX before conducting the X-ray microanalyzer quantitative analysis. Sample 9, as synthesis 2316 from Table 1 with specific surface of $31.61 \text{ m}^2 \text{ g}^{-1}$, was subjected to this type of investigations.

The analysis displayed that as result of the lithium intercalation up to 690 mV—Fig. 4(a), the light phase is enriched in lithium at the expense of a decrease of the tin content and preservation of the copper one. The implemented quantitative determinations lead to a dark phase with content LiCu_2Sn_5 and a light one with content LiCuSn_2 .

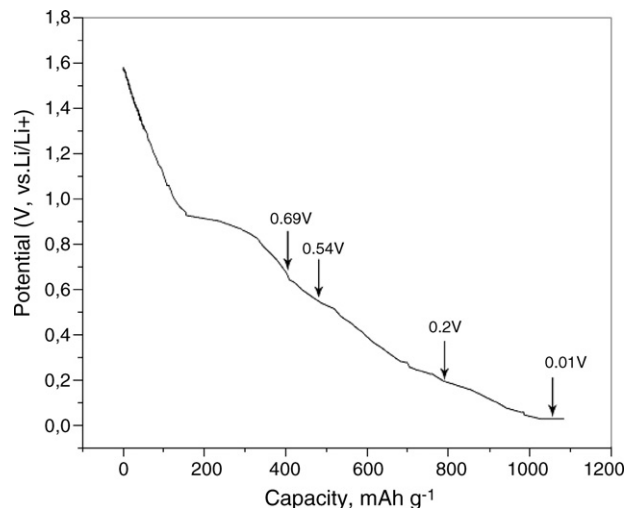


Fig. 3. Voltage profile for the first charge of $\text{Cu}_6\text{Sn}_5(\text{B})$ electrode (sample 9, synthesis #2316, Table 1) during lithiation.

By analyzing with the same technique the electrode after lithium intercalation to 540 mV—Fig. 4(b), it was established that lithium preserved its concentration equal to the one in the preceding richer in lithium light phase, copper increased, tin decreased a bit and the content $\text{LiCu}_{1.6}\text{Sn}_{2.2}$ was reached. Here, the hypothesis for a complete transition of the initial hexagonal η' Cu_6Sn_5 phase after lithium intercalation to the cubic $\text{Li}_n\text{Cu}_x\text{Sn}_y$ one, i.e. for this case to the homogeneous $\text{LiCu}_{1.6}\text{Sn}_{2.2}$, could be convincingly stated.

Applying this methodology to the next experiment, i.e. interruption of the first charge and the process of lithiation at 200 mV (Fig. 4(c)), we obtained once more quantitative estimation for the lack of change in lithium absolute concentration in the electrode. However, tin content increases many times and copper content decreases drastically and two compositionally different phases are observed. The quantitative reports showed the presence of the phase LiSn_4 or of the $\text{LiCu}_{0.3}\text{Sn}_{3.7}$ one.

In case of interruption of the first charge or lithiation of the electrode, prepared from Cu_6Sn_5 nanoparticles to 10 mV (Fig. 4(d)) a double increase by absolute value of the lithium content in the sample was observed. Phase homogenization of the electrode was again estimated, while there was increase in the copper content and decrease of the tin one. The quantitative estimations lead to content $\text{LiCu}_{0.65}\text{Sn}_{1.05}$.

The presented investigations and data in Fig. 4(b and d) are very similar both quantitatively and qualitatively. But in the case of the sample from Fig. 4(d) the lithium content is twice bigger and the copper and tin content, respectively, is twice smaller from the one of the electrode presented in Fig. 4(b).

The performed electrochemical tests in a cycling mode are presented in Fig. 5. Both the presented here results and published by us in Refs. [9,10] and by other authors [5]

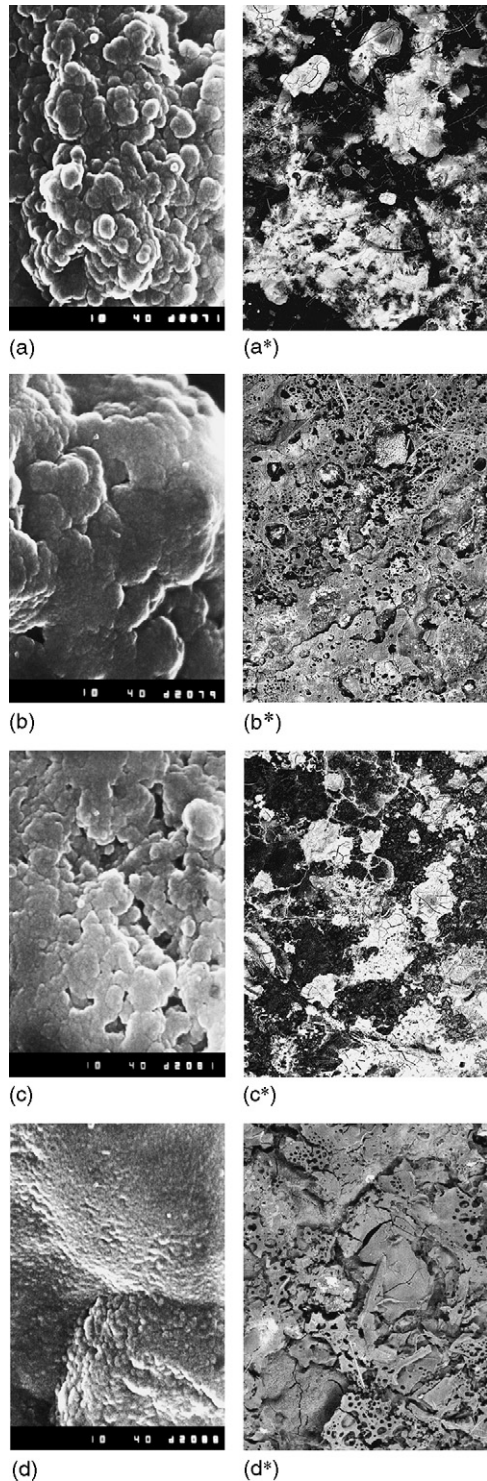


Fig. 4. (a) SEM ($\times 40,000$) and (a^{*}) EDAX image of $\text{Li}_x\text{Cu}_y\text{Sn}_z$ electrode after lithiation to 0.69 V, experimentally estimated compositions close to: LiCu_2Sn_5 , LiCuSn_2 ; (b) SEM ($\times 40,000$) and (b^{*}) EDAX image of $\text{Li}_x\text{Cu}_y\text{Sn}_z$ electrode after lithiation to 0.54 V, experimentally estimated compositions close to: $\text{LiCu}_{1.6}\text{Sn}_{2.2}$; (c) SEM ($\times 40,000$) and (c^{*}) EDAX image of $\text{Li}_x\text{Cu}_y\text{Sn}_z$ electrode after lithiation to 0.2 V, experimentally estimated compositions close to: LiSn_4 (more precisely $\text{LiCu}_{0.3}\text{Sn}_{3.7}$); (d) SEM ($\times 40,000$) and (d^{*}) EDAX image of $\text{Li}_x\text{Cu}_y\text{Sn}_z$ electrode after lithiation to 0.01 V, experimentally estimated compositions close to: $\text{LiCu}_{0.65}\text{Sn}_{1.05}$.

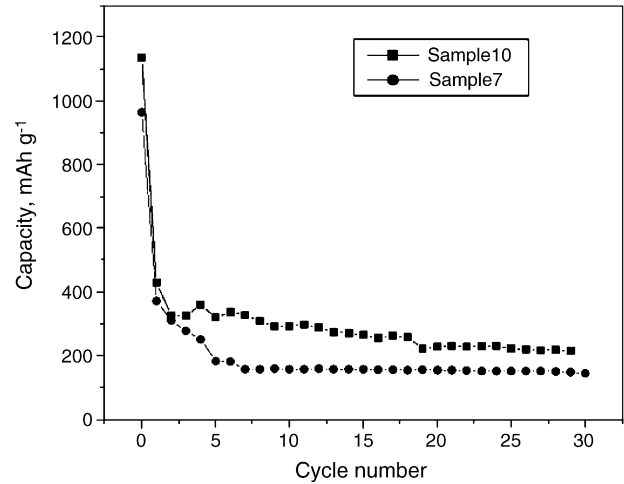


Fig. 5. Capacity vs. cycle number plots for $\text{Li}_x\text{Cu}_6\text{Sn}_5(\text{B})$ cells for voltage range 1.3–0.01 V, at a current corresponding to $C/10$.

similar ones show unambiguously the good cycleability of the nanosize materials [4].

4. Discussion

Developing the synthesis and applications of nanosize materials the researchers more and more frequently have to look for non-traditional decisions to create new devices. Nevertheless, very often the predominant explanations are well forgotten and nonetheless well known from long ago theoretical postulates and dependencies [11].

Depending on their positions the atoms are differently bound to the crystal surface. Thus, an atom adsorbed on the crystal surface is bound by one bond to the crystal and has five unsaturated dangling bonds. On the contrary, an atom incorporated into the face has five of its bonds saturated and one unsaturated. The only exception is the atom in kink-position. As is seen an atom in this position is bound to a half-atomic row, half-crystal plane and half-crystal block. By repetitive attachment or detachment of atoms to and from this position the whole crystal can be built up or disintegrated into single atoms [11].

The work $\varphi_{1/2}$ necessary to detach an atom from a half-crystal position depends on the symmetry of the crystal lattice – the number of the first, second and third neighbors of an atom in a half-crystal position and their wave electron functions: ψ_1 , ψ_2 , ψ_3 , respectively.

Thus from a Kossel' theory for metal crystal follows [11]:

$$(hcp) \text{ hexagonal closed packed} - \varphi_{1/2} = 6\psi_1 + 3\psi_2 + 1\psi_3$$

$$(fcc) \text{ face-centered cubic} - \varphi_{1/2} = 6\psi_1 + 3\psi_2 + 12\psi_3$$

It is clear that transition from a hexagonal lattice to a face-centered cubic one could be conducted without volume changes into or by destruction of the metal lattice. Its

stability is based primarily on the first and second neighboring atoms. Thus, only by change in the number of the third neighboring atoms at charge—lithium intercalation and discharge—via decrease in the number of the third neighboring atoms, reversible change transitions can be conducted. At discharge the number of the third (lithium) atoms should be decreased and the hexagonal closed pack has to be reconstructed.

Equality in the number of the first and second neighboring atoms is observed only for these two symmetric classes. It is reasonable to discuss the use of impulse modes of charge/discharge and for this working system such announcements have already started to appear.

Using nanosize materials, which obviously do not have diffusion limitations, we have to carefully select the modes of lithium intercalation, to achieve maximum precision in the intermetallic compositions content and to obtain a technological product with high capacity and exceptional cycleability by means of elementary technological equipment, operating at room temperature and atmospheric pressure.

Acknowledgement

This work has been supported by the National Science Foundation of USA as Joint Project INT #0124080 between

Kansas State University and Bulgarian Academy of Sciences, Institute of Electrochemistry and Energy Systems.

References

- [1] K.D. Kepler, J.T. Vaughey, M.M. Thackeray, *Electrochem. Solid State Lett.* 2 (7) (1999) 307.
- [2] D. Larcher, L.Y. Beaulieu, D.D. MacNeil, J.R. Dahn, *J. Electrochem. Soc.* 147 (5) (2000) 1658.
- [3] J. Yang, Y. Takeda, N. Imanishi, O. Yamamoto, *J. Electrochem. Soc.* 146 (11) (1999) 4009.
- [4] J. Yang, M. Wachtler, M. Winter, J.O. Besenhard, *Electrochem. Solid State Lett.* 2 (4) (1999) 161.
- [5] D.G. Kim, H. Kim, H.-J. Sohn, T. Kang, *J. Power Sources* 104 (2002) 223–225.
- [6] K.J. Klabunde (Ed.), *Nanoscale Materials in Chemistry*, John Wiley & Sons Inc., USA, 2001.
- [7] I.D. Dragieva, Z.B. Stoynov, K.J. Klabunde, *Scripta Mater.* 44 (2001) 2187.
- [8] I. Dragieva, C. Deleva, M. Mladenov, I. Markova-Deneva, *Monatshefte fuer Chemie, Chem. Monthly* 133 (2002) 807.
- [9] M. Mladenov, P. Zlatilova, E. Lefterova, I. Dragieva, *J. Univ. Chem. Technol. Metall., Bulgaria*, XXXVIII 2 (2003) 529.
- [10] M. Mladenov, P. Zlatilova, S. Vassilev, Tz. Iliev, I. Dragieva, K. Klabunde, *Sixth National Workshop Nanoscience & Nanotechnology*, Sofia, Bulgaria, November 24–27, 2004, p. 117 (Abstract).
- [11] I. Markov, *Crystal Growth for Beginners: Fundamentals of Nucleation, Crystal Growth, and Epitaxy*, second ed., World Scientific Publishers, Singapore, 2003, p. 40.